Supporting Information

Construction of porphyrin-based conjugated microporous polymer through quaternization for efficient photodegradation of tetracycline and bisphenol A

Jianan Fan[a]†, Qingxia Zhu[b]†, Haoxi Wang[b], Po Sun[a,e], Lingyun Xu[c],* Hua Sun[d],* Shiyuan Zhou[b], Peiyang Gu[b]**

[a]Institutes of Molecular Engineering and Applied Chemistry, Analysis and Testing Central Facility, Anhui University of Technology, Ma'anshan 243002, P. R. China. E-mail address: sunpoo@ahut.edu.cn (P. Sun);

[b]Jiangsu Key Laboratory of Advanced Catalytic Materials and Technology, School of Petrochemical Engineering, Changzhou University, Changzhou, 213164, PR China. E-mail address: gupeiyang0714@cczu.edu.cn (P. Gu);

[c]Analysis and Testing Center, Soochow University, Suzhou, 215123, China. E-mail address: lyxu@suda.edu.cn (L. Xu);

[d]School of Material and Chemistry Engineering, Xuzhou University of Technology, Xuzhou, 221018, China. E-mail: iamsunhua@xzit.edu.cn (H. Sun);

[e]MaAnShan High-Tech Research Institute of Nanjing University, MaAnShan 238200, P. R. China.

Contents

1. Characterization

The FT-IR and ss ^{13}C NMR spectra of the samples were recorded using a Nicolet 6700 Fourier Transform Infrared Spectrometer (Thermo Scientific, USA) and a Bruker INOVA 400 MHz NMR Spectrometer, respectively. The surface chemical properties of the catalyst were analyzed using X-ray photoelectron spectroscopy (XPS, ESCALAB 250, USA). The UV-Vis diffuse reflectance spectra (UV-Vis DRS) were measured using a U-3010 spectrometer (Hitachi, Japan). The surface morphologies of Por-BT-1 and Por-BT-2 were characterized by scanning electron microscopy (SEM, Merlin Compact, Japan). The BET surface area and pore size distribution were recorded by nitrogen adsorption-desorption isotherms at 77 K using a Micromeritics ASAP 2020 surface area analyzer. The thermal stability of the samples was evaluated by thermogravimetric analysis (TGA, TG209F3, Germany) with a heating rate of 10°C min^{-1} from 30°C to 700°C. The contact angle of the samples was measured using a droplet shape analyzer (Kruss, DSA25). The concentration of TC in aqueous solutions was analyzed by UV-Vis spectrophotometry (METASH X-8S, China), while the concentrations of BPA, BPAF, BPF, and BPS in solutions were determined by high-performance liquid chromatography (HPLC, Fuli LC5090, China). The photoelectrochemical properties of the catalysts were measured using a CHI760E electrochemical workstation (Chenhua, China). Radicals were detected by electron spin resonance spectroscopy (Bruker ESR 5000, Germany), and the total organic carbon (TOC) content was measured using a multi N/C analyzer (analytik-jena multi N/C 2100S, Germany). Reaction intermediates were analyzed by liquid chromatography-

mass spectrometry (LC-MS, Agilent 8860, California, USA).

2. Synthetic procedure

The synthetic procedures of Por-BT-1 and Por-BT-2 are shown in the manuscript.

Synthesis of Por-BT-L：5,10,15,20-Tetra(4-bromophenyl) porphyrin (0.20 g, 0.20 mmol), 4,7-bis(4,4,5,5-tetramethyl-1,3,2-dioxaborolan-2-yl)-2,1,3-benzothiadiazole (0.04 g, 0.10 mmol), and tetrabutylammonium iodide (0.01 g, 0.06 mmol) were dissolved in 20 mL of 1,4-dioxane in a 100 mL Schlenk flask under a N_2 atmosphere. 1.40 mL of K_2CO_3 aqueous solution (2 M) was then added, followed by the addition of tetrakis(triphenylphosphine)palladium (0.03 mg, 0.02 mmol) with continuous N_2 flow. The reaction was heated to 110 °C and stirred for 3 d. The mixture was then cooled to room temperature and filtered. The solid residue was extracted with methanol, dichloromethane, and tetrahydrofuran using a Soxhlet extractor, followed by drying in a vacuum oven at 60 °C to afford 0.06 g of Por-BT-L with a yield of 53.6%.

Synthesis of Por-BT-M：5,10,15,20-Tetra(4-bromophenyl) porphyrin (0.20 g, 0.20 mmol), 4,7-bis(4,4,5,5-tetramethyl-1,3,2-dioxaborolan-2-yl)-2,1,3-benzothiadiazole (0.31 g, 0.80 mmol), and tetrabutylammonium iodide (0.01 g, 0.06 mmol) were dissolved in 20 mL of 1,4-dioxane in a 100 mL Schlenk flask under a N_2 atmosphere. 1.40 mL of K_2CO_3 aqueous solution (2 M) was then added, followed by the addition of tetrakis(triphenylphosphine)palladium (0.03 mg, 0.02 mmol) with continuous N_2 flow. The reaction was heated to 110 °C and stirred for 3 d. The mixture was then cooled to room temperature and filtered. The soli d residue was extracted with methanol, dichloromethane, and tetrahydrofuran using a Soxhlet extractor,

followed by drying in a vacuum oven at 60 °C to afford 0.18 g of Por-BT-M with a yield of 67.6%.

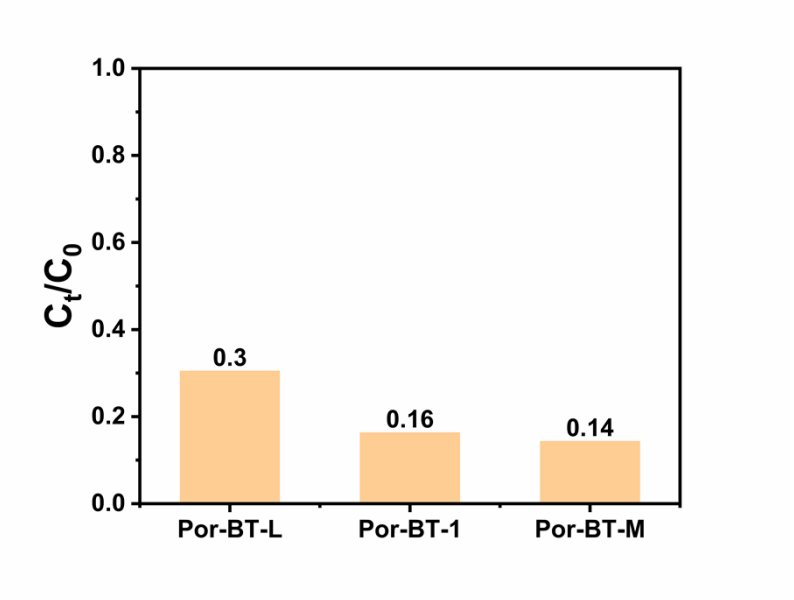

Fig. S1 Comparative schematic of TC degradation by three photocatalysts prepared at different reactant ratios.

3. Photoelectrochemical characterization

For the measurement of Mott-Schottky plots, transient photocurrent response, and electrochemical impedance spectroscopy (EIS), a three-electrode system was used. The working electrode was prepared by dropping 200 μL of the mixture onto an ITO glass substrate (1 cm × 2 cm × 0.1 cm). An Ag/AgCl electrode was used as the reference electrode, and a platinum sheet served as the counter electrode. The measurements were conducted in a 0.1 M sodium sulfate aqueous solution. A suspension was prepared by dispersing 5 mg of the sample in 1 mL of ethanol containing 20 μL of Nafion solution, followed by sonication. A 300 W xenon lamp was employed as the light source for the photoelectrochemical tests.

4. Radical detection

To investigate the photocatalytic degradation properties, 10 mg of Por-BT-1 was dispersed in 20 mL of TC solution (10 ppm). Sodium ethylenediaminetetraacetate (EDTA-2Na) (8 mg) was added to scavenge holes (h^+). The solution was then irradiated with a·300W·xenon lamp. Following this, the procedures were the same as those used in the aforementioned photocatalytic degradation experiments. Similarly, β-carotene (8 mg) was added to scavenge singlet oxygen ($^1O_2$). In a separate experiment, 10 mg of Por-BT-1 was dispersed in 19.8 mL of TC solution (10 ppm), with 200 μL of isopropanol (IPA, AR, 99.5%) added to scavenge hydroxyl radicals (•OH). For the scavenging of superoxide radicals ($•O_2^-$), 10 mg of Por-BT-1 was dispersed in 19.6 mL of TC solution (10 ppm), and 400 μL of a TEMPO solution (1 g/L) was added.

To assess the photocatalytic activity, 5 mg of Por-BT-2 was dispersed in 10 mL of BPA solution (10 ppm). Sodium EDTA-2Na (4 mg) was added to scavenge h^+, and the solution was subsequently irradiated with a·300W·xenon lamp. The subsequent steps followed the same procedures as those used in the previously described photocatalytic degradation experiments. Similarly, β-carotene (4 mg) was added to scavenge $^1O_2$. In another experiment, 5 mg of Por-BT-2 was dispersed in 9.9 mL of BPA solution (10 ppm), with 100 μL of IPA, (AR, 99.5%) added to scavenge •OH. For scavenging $•O_2^-$, 5 mg of Por-BT-2 was dispersed in 9.8 mL of BPA solution (10 ppm), and 200 μL of a p-Benzoquinone (p-BQ) solution (1 g/L) was added.

5. Degradation pathways

Analysis was performed using a high-performance liquid chromatography coupled with a single quadrupole mass spectrometer (LC-MS). For the detection of degradation

intermediates of TC, a gradient elution was carried out using a 0.1% (v/v) formic acid aqueous solution (A) and acetonitrile (B) as mobile phases. The flow rate was set at 0.3 mL/min with an injection volume of 20 μL, and the column temperature was maintained at 30°C. The analysis was conducted in negative electrospray ionization (ESI^-) mode.

For the detection of BPA degradation intermediates, a mixture of ultrapure water and methanol (v/v=30/70) was used as the mobile phase, with a flow rate of 1 mL/min and an injection volume of 20 μL. The column temperature was set to 35°C, and the analysis was performed in negative electrospray ionization (ESI^-) mode.

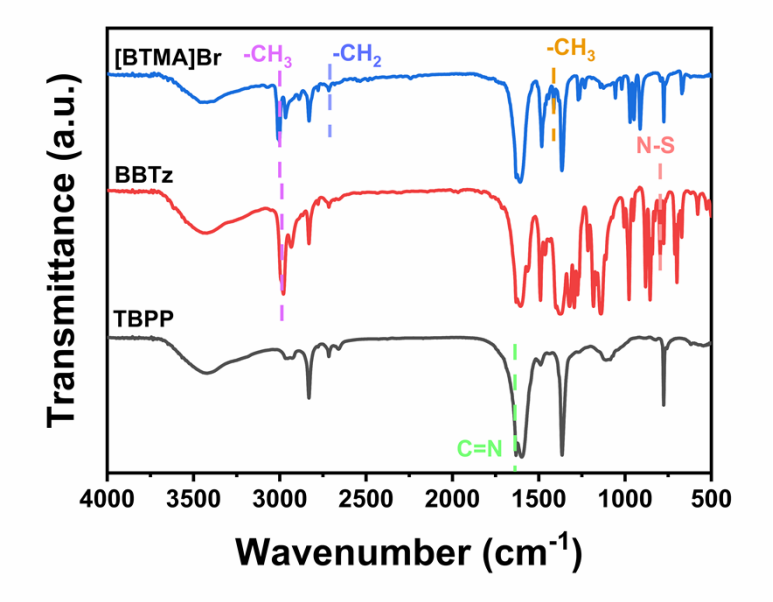

Fig. S2 FT-IR spectra of TBPP, BBTz and [BTMA]Br. (TBPP: 5,10,15,20-tetrakis(4-bromophenyl)porphyrin, BBTz: 4,7-bis(4,4,5,5-tetramethyl-1,3,2-dioxaborolan-2-yl)benzo[c][1,2,5]thiadiazole, [BTMA]Br: (2-Bromoethyl)trimethylammonium bromide)

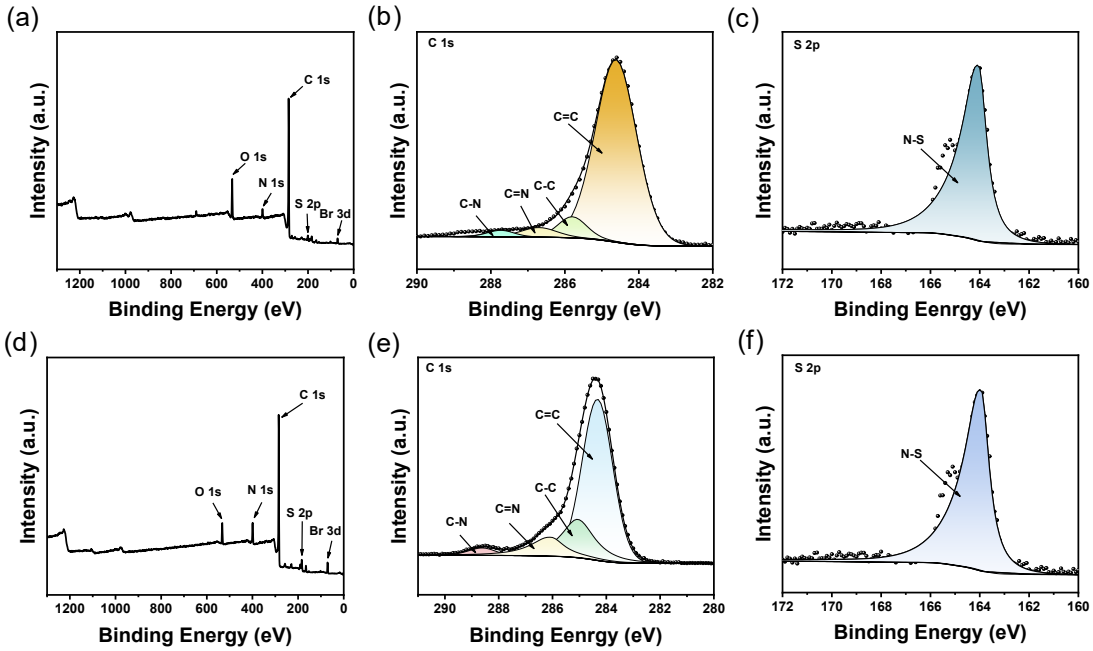

Fig. S3 The full XPS spectra, C 1s and S 2p high-resolution XPS spectra of (a-c) Por-BT-1 and (d-f) Por-BT-2.

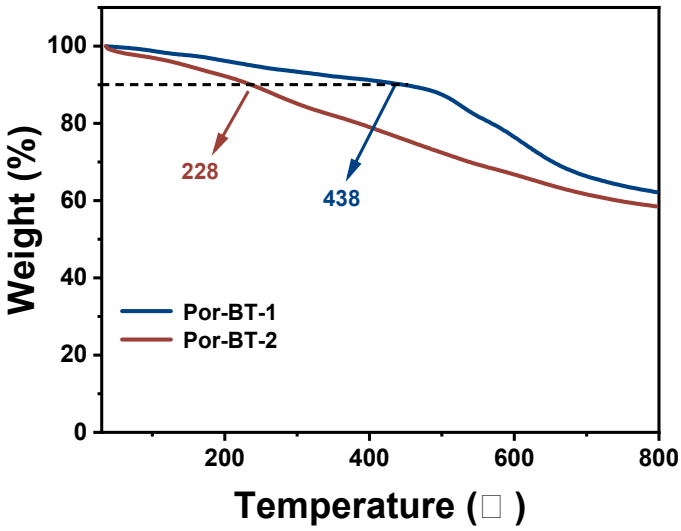

Fig. S4 The TGA curves of Por-BT-1 and Por-BT-2.

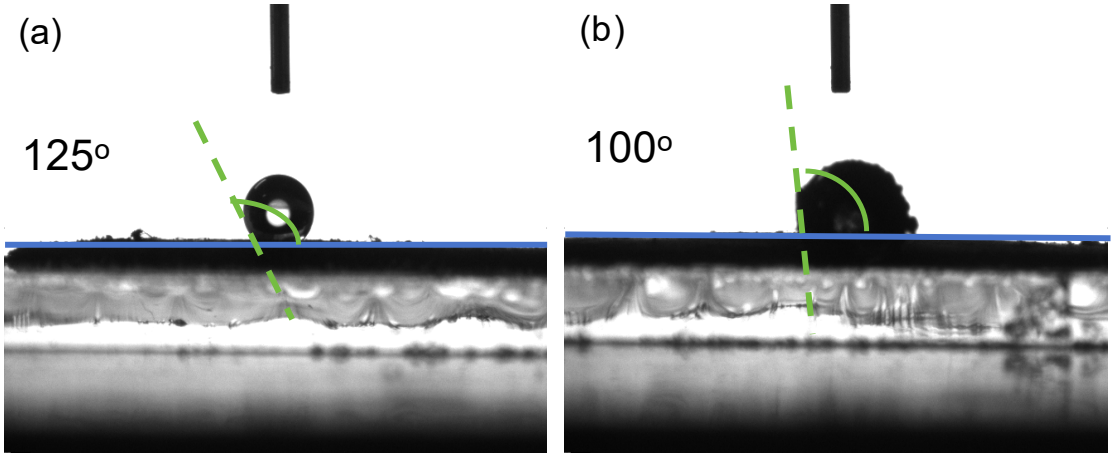

Fig. S5 The water contact angles of Por-BT-1 and Por-BT-2.

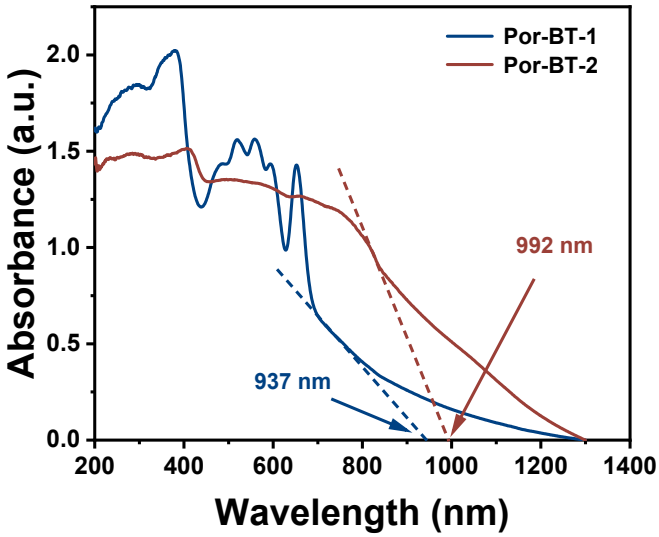

Fig. S6 The UV-vis diffuse reflectance absorption spectra of Por-BT-1 and Por-BT-2.

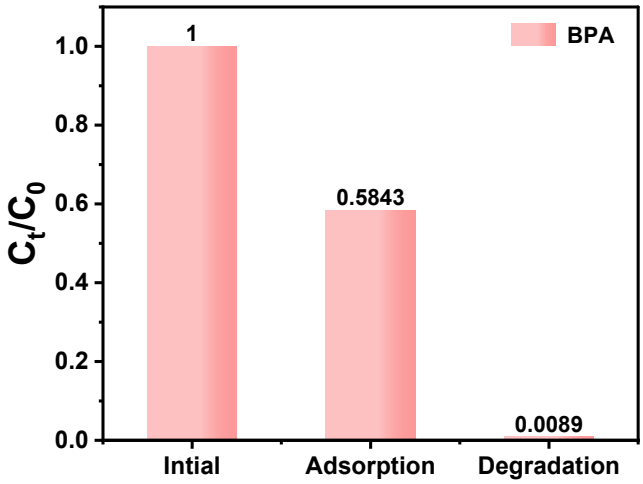

Fig. S7 The percentage of BPA residues in Por-BT-2 after dark adsorption and photocatalytic degradation.

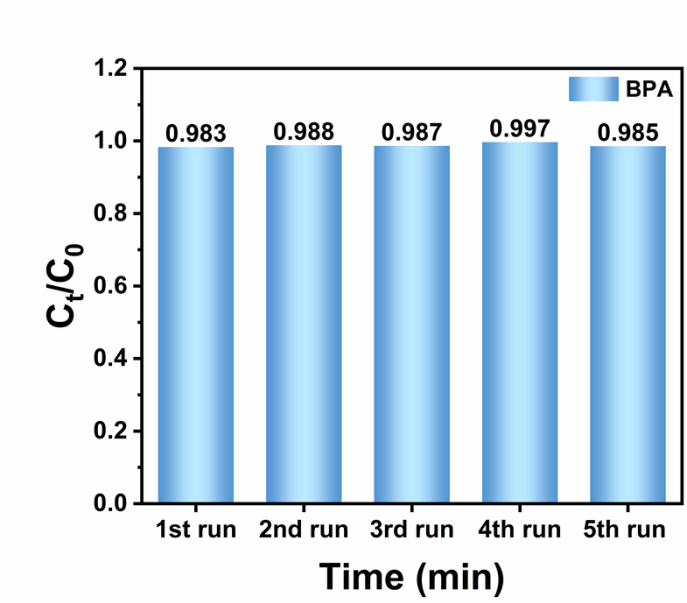

Fig. S8 Photocatalytic reusability of Por-BT-2 in BPA degradation through five runs.

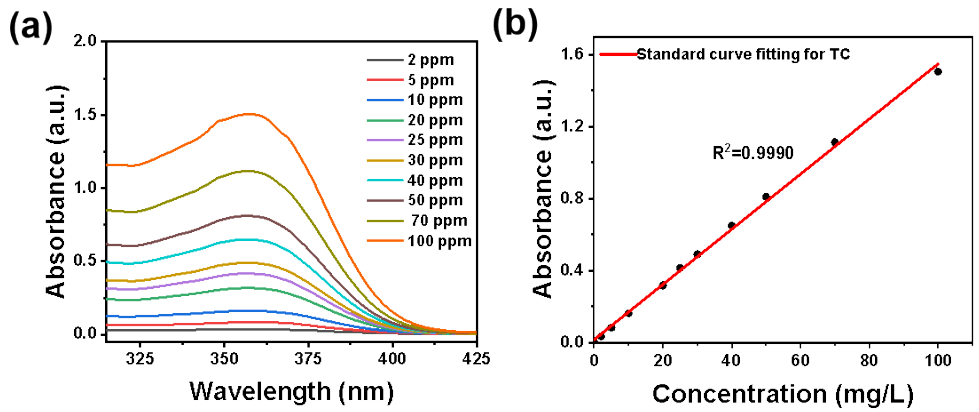

Fig. S9 (a) The absorbance spectra of TC with different concentrations; (b) the corresponding standard curve.

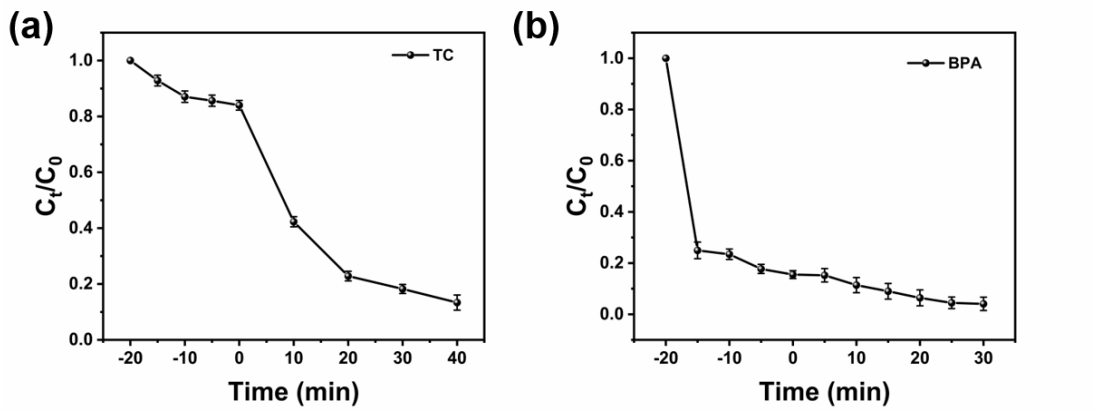

Fig. S10 (a) The photocatalytic degradation performance of TC and (b) BPA.

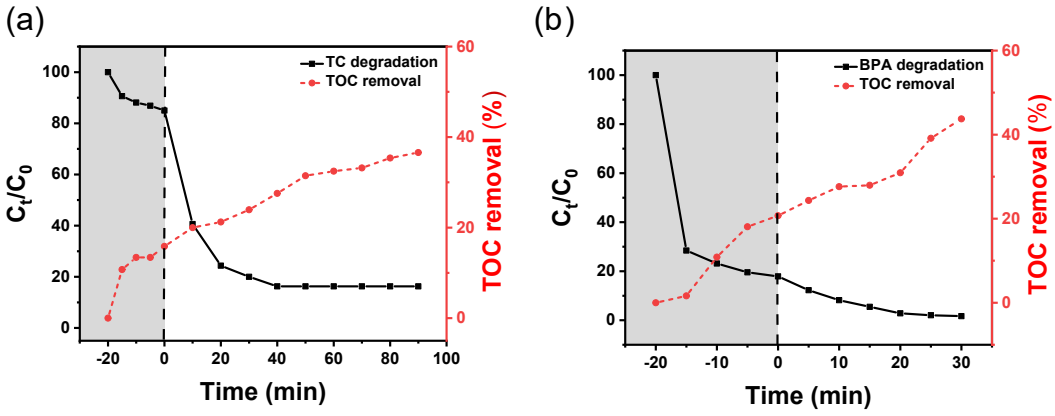

Fig. S11 The residual rate of total organic carbons for Por-BT-1 in the removal of TC (10 ppm) and Por-BT-2 in the removal of BPA (10 ppm).

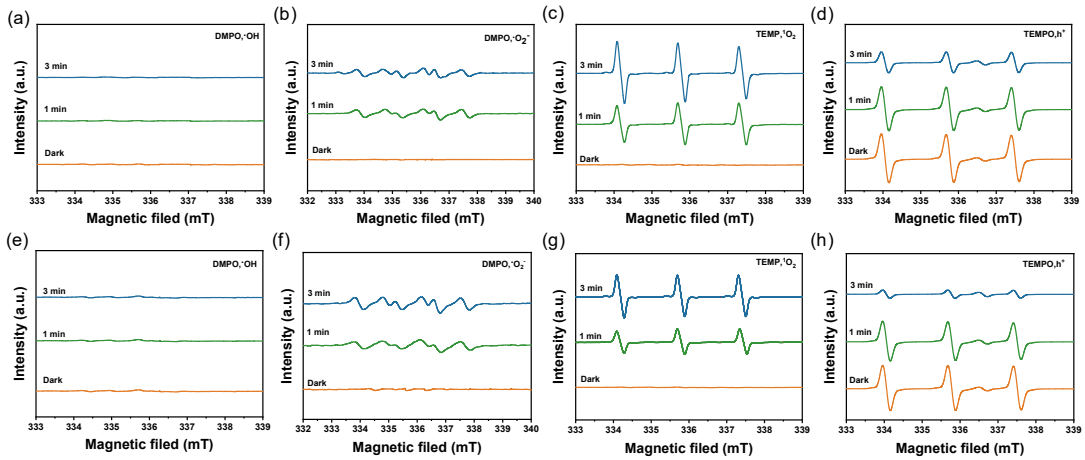

Fig. S12 The ESR spectra of DMPO–•OH, DMPO–•O_2^-, TEMP–$^1O_2$, and TEMPO–h^+ for (a-d) Por-BT-1 and (e-h) Por-BT-2 in the dark and under visible-light irradiation.

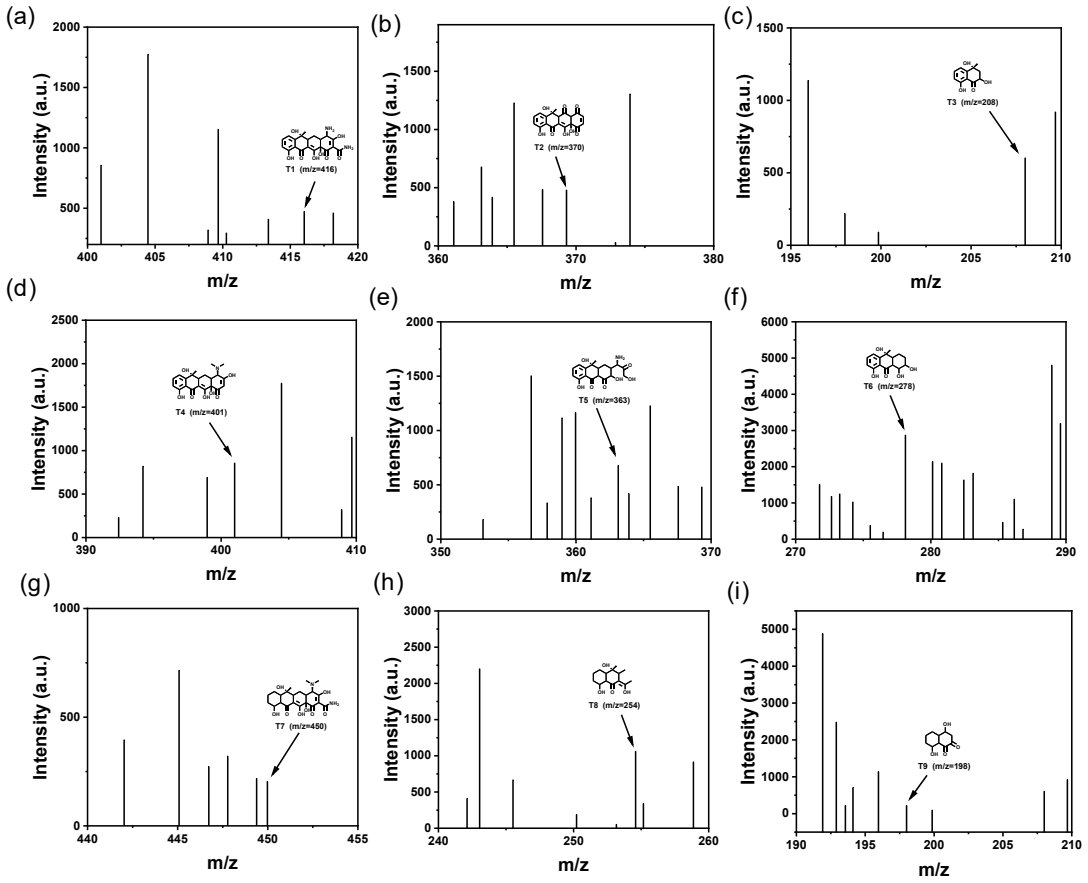

Fig. S13 The LC-MS results of the photodegradation pathway of Por-BT-1 toward TC.

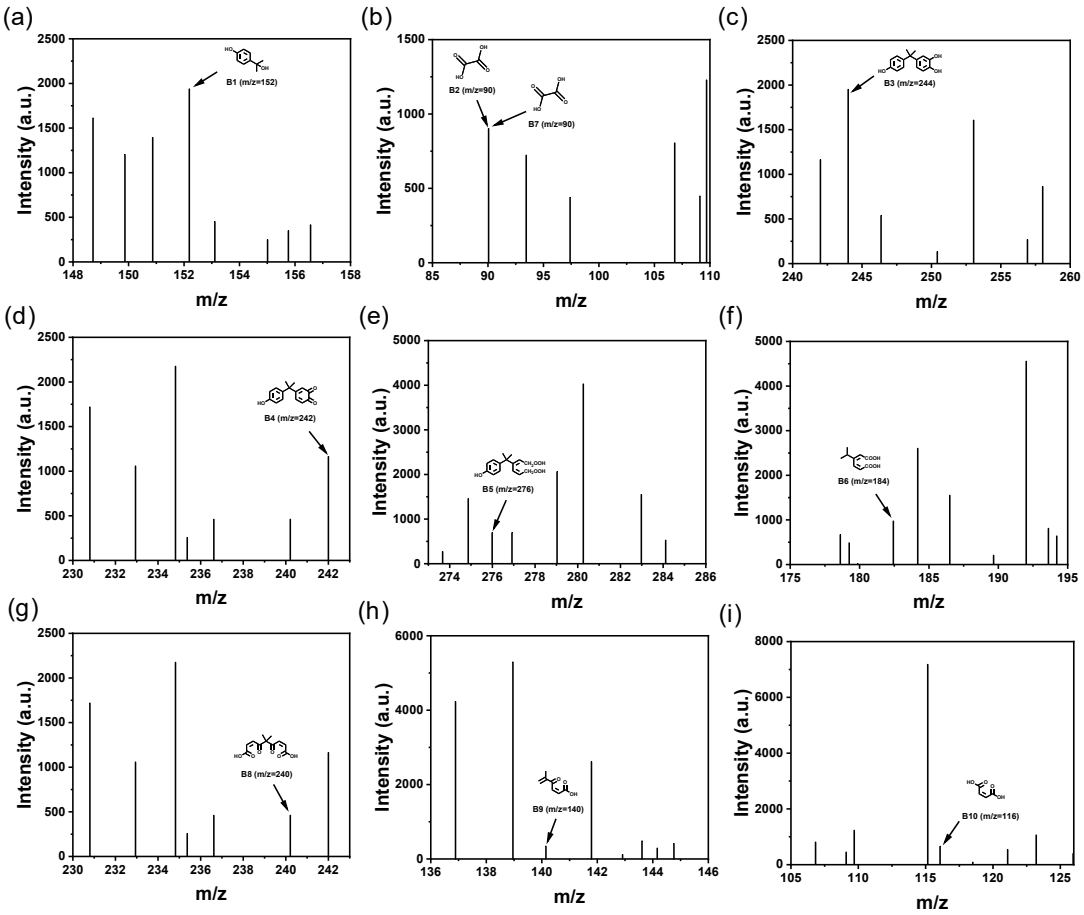

Fig. S14 The LC-MS results of the photodegradation pathway of Por-BT-2 toward BPA.

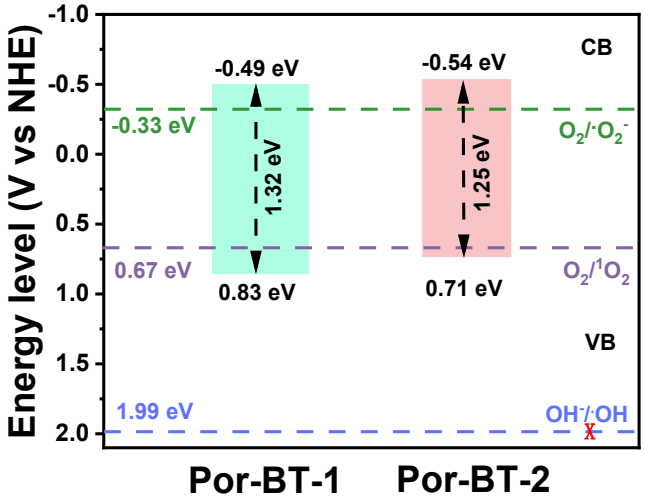

Fig. S15 The band gaps of Por-BT-1 and Por-BT-2.

Table S1 The surface areas and pore volumes of Por-BT-1 and Por-BT-2.

Sample	BET surface area S_{BET} (m^2 g^{-1})	Total pore valume (cm^3 g^{-1})	Pore size distribution (nm)
Por-BT-1	74.37	0.13	6.73
Por-BT-2	190.08	0.17	2.8

Table S2. Comparison of efficiency of removing BPA by different catalysts.

Catalysts	Dosage (g L^{-1})	C_{BPA} (ppm)	Time (min)	Efficiency (%)	Reference
Pristine TiO_2	1	2.5	60	22	1
Nano PDI	0.5	5	480	94	2
g-C_3N_4NS+PS	0.5	5	90	10	3
π-conjugated-PDI	0.5	5	120	99.7	4
SKA-CN	0.3	~10	100	98	5
Co-MiL-53-NH_2-BT	0.25	10	120	99.9	6
OCN 6	0.2	10	120	98.68	7
PDINH	0.5	10	480	82	8
g-C_3N_4	1	10	180	30	9
Por-BT-2	**0.5**	**10**	**30**	**98.3**	**This work**

Table S3. Comparison of efficiency of removing TC by different catalysts.

Catalysts	Dosage (g L^{-1})	C_{TC} (ppm)	Time (min)	Efficiency (%)	Reference
Bi_2S_3/MIL-53(Fe)	0.1	10	180	90.9	10
Mn-$SrTiO_3$	1	10	60	66.7	11
Ag_3PO_4/$CuBi_2O_4$	0.5	10	60	75	12
$Bi_2O_2CO_3$/Ti_3C_2	0.5	20	120	31	13
CuPT-CPP	0.25	10	210	100	14
Ag@MOF-525	0.4	10	200	81	15

Py-NH_2–COF	0.2	10	90	3.1	16
Por-BT-1	**0.5**	**10**	**40**	**83.7**	**This work**

References

1. Xu, L.; Yang, L.; Johansson, E. M. J.; Wang, Y.; Jin, P., *Chem. Eng. J.* 2018, **350**, 1043-1055.

2. Wang, J.; Shi, W.; Liu, D.; Zhang, Z.; Zhu, Y.; Wang, D., *Appl. Catal., B.* 2017, **202**, 289-297.

3. Liu, B.; Qiao, M.; Wang, Y.; Wang, L.; Gong, Y.; Guo, T.; Zhao, X., *Chemosphere.* 2017, **189**, 115-122.

4. Zhang, Y.; Wang, D.; Liu, W.; Lou, Y.; Zhang, Y.; Dong, Y.; Xu, J.; Pan, C.; Zhu, Y., *Appl. Catal., B.* 2022, **300**, 120762.

5. Xu, L.; Li, L.; Yu, L.; Yu, J. C., *Chem. Eng. J.* 2022, **431**, 134241.

6. Lv, S.-W.; Liu, J.-M.; Zhao, N.; Li, C.-Y.; Wang, Z.-H.; Wang, S., *J. Hazard. Mater.* 2020, **387**, 122011.

7. Long, X.; Feng, C.; Yang, S.; Ding, D.; Feng, J.; Liu, M.; Chen, Y.; Tan, J.; Peng, X.; Shi, J.; Chen, R., *Chem. Eng. J.* 2022, **435**, 134835.

8. Liu, D.; Wang, J.; Bai, X.; Zong, R.; Zhu, Y., *Adv. Mater.* 2016, **28**, 7284-7290.

9. Jing, L.; Wang, D.; He, M.; Xu, Y.; Xie, M.; Song, Y.; Xu, H.; Li, H., *J. Hazard. Mater.* 2021, **401**, 123309.

10. Xie, J.; Tang, Y.; Chen, F.; Hao, C. C., *J. Phys. Chem. Solids.* 2023, **181**, 111551.

11. Wu, G.; Li, P.; Xu, D.; Luo, B.; Hong, Y.; Shi, W.; Liu, C., *Appl. Surf. Sci.* 2015, **333**, 39-47.

12. Shi, W.; Guo, F.; Yuan, S., *Appl. Catal., B.* 2017, **209**, 720-728.

13. Tan, B.; Fang, Y.; Chen, Q.; Ao, X.; Cao, Y., *J. Colloid Interface Sci.* 2021, **601**, 581-593.

14. Xu, Z.; Dong, W.; Cui, X.; Duan, Q., *Chemosphere.* 2024, **355**, 141801.

15. Guo, A.; Wang, X.; Liu, H.; Li, X.; Yang, L.; Yang, W., *Surf. Interfaces.* 2023, **38**, 102843.

16. Hu, Z.; Luo, Y.; Wang, L.; Wang, Y.; Wang, Q.; Jiang, G.; Zhang, Q.; Cui, F., *ACS Appl. Polym. Mater.* 2023, **5**, 9263-9273.